Physiological and Ultrastructural Analysis of Elongating Mitotic Spindles Reactivated In Vitro

W. Zacheus Cande and Kent McDonald

Department of Botany, University of California, Berkeley, California 94720

Abstract. We have developed a simple procedure for isolating mitotic spindles from the diatom *Stephanopyxis turris* and have shown that they undergo anaphase spindle elongation in vitro upon addition of ATP. The isolated central spindle is a barrel-shaped structure with a prominent zone of microtubule overlap. After ATP addition >75% of the spindle population undergoes distinct structural rearrangements: the spindles on average are longer and the two half-spindles are separated by a distinct gap traversed by only a small number of microtubules, the phase-dense material in the overlap zone is gone, and the peripheral microtubule arrays have depolymerized. At the ultrastructural level, we examined serial cross-sections of spindles after 1-, 5-, and 10-min incubations in reactivation medium. Microtubule depolymerization distal to the poles is confirmed by the increased number of incomplete, i.e., c-microtubule profiles specifically located in the region of overlap. After 10 min we see areas of reduced microtubule number which correspond to the gaps seen in the light microscope and an overall reduction in the number of half-spindle microtubules to about one-third the original number. The changes in spindle structure are highly specific for ATP, are dose-dependent, and do not occur with nonhydrolyzable nucleotide analogues. Spindle elongation and gap formation are blocked by 10 μM vanadate, equimolar mixtures of ATP and AMPPNP, and by sulfhydryl reagents. This process is not affected by nocodazole, erythro-9-[3-(2-hydroxynonyl)]adenine, cytochalasin D, and phalloidin. In the presence of taxol, the extent of spindle elongation is increased; however, distinct gaps still form between the two half-spindles. These results show that the response of isolated spindles to ATP is a complex process consisting of several discrete steps including initiation events, spindle elongation mechanochemistry, controlled central spindle microtubule plus-end depolymerization, and loss of peripheral microtubules. They also show that the microtubule overlap zone is an important site of ATP action and suggest that spindle elongation in vitro is best explained by a mechanism of microtubule–microtubule sliding. Spindle elongation in vitro cannot be accounted for by cytoplasmic forces pulling on the poles or by microtubule polymerization.

THE development of an in vitro system for analyzing anaphase chromosome movement is essential for understanding the molecular basis of mitosis. Studies of the mechanism of glycerinated myofibril contraction provide a clear example of how physiological, morphological, and biochemical analyses of a model system can lead to an understanding of a contractile process at a molecular level (1, 41). Unfortunately, an in vitro analysis of mitosis has not been very successful, since spindles isolated from the most readily available sources, such as sea urchin eggs or mammalian tissue culture cells, are nonfunctional (58) (for possible exceptions, see references 16, 44, and 45) and these spindles lack the exquisite molecular ordering of the filament systems found in striated muscle. Another and potentially more serious problem is that the mechanochemistry of the mitotic spindle may be more complex than that of muscle (19, 40). Physiological studies of permeabilized cell models (8, 9, 11, 12) and drug studies of living cells (35, 43) suggest that at least two motors are involved; one to move chromosomes to the poles (anaphase A) and one to separate the spindle poles (anaphase B). In many spindles (for example, the mammalian spindle) the machinery responsible for anaphase A and B are mixed together and these processes occur at the same time. In addition, other mechanochemical systems may be present to reposition the re-forming nuclei at the end of anaphase (3, 40, 56) or to move chromosomes during prometaphase congression (34, 49).

Diatom spindles have been important model systems for describing the morphological changes associated with anaphase chromosome movement because the fibrous systems responsible for anaphase A and B are spatially separated (38) and the central spindle is a paracrystalline array of microtubules (28, 29). The diatom central spindle is constructed of two sets of interdigitating microtubules that originate from plate-like spindle poles (38) and display specific near-neighbor interactions in the zone of microtubule overlap

(28). This overlap zone is visible even with a light microscope (39) and decreases as the central spindle elongates during anaphase B (29, 39). We reasoned that the structural properties that make diatom spindles so useful for morphological studies would also be advantageous for developing an in vitro model system for studying anaphase chromosome movement.

Recently, we have developed a method for isolating spindles from dividing cells of the centric diatom *Stephanopyxis turris* and have shown with video microscopy that these spindles undergo anaphase spindle elongation in vitro (10). With the addition of ATP, the two half-spindles slide completely apart with a concurrent decrease in the extent and magnitude of birefringence of the overlap zone (10). In this paper we describe the conditions for isolating functional central spindles and we characterize the ultrastructure of isolated spindles before and after reactivation with ATP. Since over three-quarters of the spindles on a coverslip show distinct midzone structural changes after ATP-dependent reactivation, we have developed a simple assay based on immunofluorescence and light microscopy for studying the physiological requirements of spindle elongation in vitro. We demonstrate that ATP causes spindles to elongate and initiates a controlled plus-end depolymerization of MTs which mimics changes in vivo (47). Spindle reactivation requires ATP hydrolysis and is highly specific for ATP, and elongation is inhibited by vanadate, sulfhydryl reagents, and by equimolar mixtures of AMPPNP and ATP. We interpret these results to mean that spindle elongation in diatoms is effected by a unique mechanochemical ATPase with some dyneinlike properties and that ATP is also required for the controlled disassembly of spindle MTs. We discuss these results in the context of currently favored models of spindle elongation.

Materials and Methods

Materials

Nucleotides, nonhydrolyzable nucleotide analogues, drugs, and enzymes were obtained from Sigma Chemical Co. (St. Louis, MO) or Boehringer-Mannheim GmbH (Mannheim, FRG). Vanadate was obtained from Accurate Chemical & Scientific Corp. (Westbury, NY). Taxol was a gift from Dr. Matthew Suffness, Natural Products Branch, Division of Cancer Treatment, National Cancer Institute, Bethesda, MD.

Cell Culture and Synchronization

Stephanopyxis turris (stock No. L1272) was obtained from the Culture Collection of Marine Phytoplankton, Bigelow Laboratory for Ocean Sciences, West Boothbay, ME. Cells were grown in F/2 medium (17) in a suspension culture on 6.5-h day, 17.5-h night schedule at 19°C. 3 h before harvest cells were drugged with 2×10^{-8} M nocodazole and 20 min before harvest cells were collected on 60-μm mesh Nitex filters, and cells were extensively washed to remove the drug. Cells were harvested by filtration at the height of the division peak which occurred 1½–2 h after night began. Using this schedule, it is routine for >50% of the cells to have undergone cell division during the division peak (56). 20 min after drug reversal all cells undergoing mitosis are at a similar stage, that is, the central spindles are 6–8-μm long and the cells are in metaphase–early anaphase.

Spindle Isolation and Reactivation

Cells were suspended in homogenization medium on ice (50 mM Pipes, pH 7.0, 40 mM sodium glycerophosphate, 10 mM $MgSO_4$, 10 mM EGTA, 0.2% Brij 58, 30% glycerol, 1 mM dithiothreitol (DTT),[1] 0.5 mM phenylmethylsulfonyl fluoride, 10 mg/liter soybean trypsin inhibitor, 10 mg/liter L-1-tosylamide-2-phenyl-ethylchloromethylketone, 10 mg/liter benzyl arginyl methyl ester, 1 mg/liter leupeptin, 1 mg/liter pepstatin), then homogenized on ice with two strokes of a Kontes dounce homogenizer, β pestle. The homogenate was filtered once through 60-μm mesh and then through 25-μm mesh Nitex filters, then centrifuged for 10 min, 0°C at 2,000 *g* onto coverslips (Fig. 1). The coverslips were placed in fresh homogenizing medium in plastic dishes and briefly swirled to remove adhering chloroplasts, then stored on ice until use. Using this procedure coverslips containing several hundred spindles can be prepared in 1–2 h. The major contaminants present are glass wall fragments, chloroplasts, and interphase nuclei. Several spindles are present in every low (25×) magnification field, and structural changes can be detected even at this low magnification.

For spindle reactivation studies, coverslips were transferred to reactivation medium (50 mM Pipes, pH 7.0, 5 mM $MgSO_4$, 10 mM EGTA, 1 mM DTT, with or without proteolytic inhibitors, and nucleotide) and incubated at room temperature or in a water bath at 20°C. Reactivation was terminated by addition of fixative, usually 3.7% formaldehyde. For the ATP concentration series, an ATP-regenerating system consisting of 0.1 mg/ml creatine kinase and 15 mM creatine phosphate was added to the reactivation medium. In some experiments 50 mM 2-(*N*-morpholino)ethane sulfonic acid, pH 6.5 was used in the homogenizing medium instead of Pipes.

Light Microscopy

Micrographs of fluorescent or phase images were made on a Zeiss Universal or photomicroscope equipped with epifluorescence optics and a 100× Neofluar or 25× Plan-neofluar lens. Unless otherwise indicated spindle lengths were measured off a TV monitor using a DAGE-MTI low-light level TV camera (DAGE-MTI Inc., Wabash, MI), and all metaphase spindles on a transect of the preparation were used for length measurements. The only spindles that were discarded were those that were not in metaphase (as defined in Results), or those whose poles were out of focus or obscured by debris.

Indirect Immunofluorescence

The antibody against tubulin (a monoclonal antibody against sea urchin flagellar tubulin) was kindly provided by Dr. David Asai (Department of Biology, Purdue University) and its preparation and characterization have been described previously (2). Spindles, fixed in 3.7% formaldehyde were washed extensively in phosphate-buffered saline (PBS), then incubated in the primary antibody for 30 min at 37°C. After extensive rinses in PBS coverslips were then incubated for a similar length of time in fluorescein-conjugated goat anti-mouse IgG (Cappel Laboratories, Cochranville, PA). Antibodies were normally used at dilutions that provided 0.1 mg/ml antibody. Coverslips were mounted in 90% glycerol, 10% PBS, 100 mg/ml 1,4 diazobicyclo-[2,2,2]octane before viewing. Chromatin was stained by adding 200 ng/ml 4′,6-diamidino-2-phenylindole dihydrochloride to the isolation or reactivation medium.

Electron Microscopy

Intact cells were prepared for electron microscopy by fixation in 0.5% glutaraldehyde in f/2 medium (17) for 30 min at 23°C (unless otherwise stated, all remaining steps were at 23°C). Spindles were rinsed for 5 min in PBS (137 mM NaCl, 2.68 mM KCl, 8 mM Na_2HPO_4-$7H_2O$, 1.47 mM KH_2PO_4) at pH 7.3, fixed in 0.2% OsO_4 + 0.3% $K_3Fe(CN)_6$ in PBS for 15 min at 4°C, rinsed twice in PBS for 5 min each, rinsed in distilled H_2O for 5 min, incubated in 2% aqueous uranyl acetate for 90 min, dehydrated in acetone by 10% steps for 10 min each, and embedded in Epon-Araldite (3.1 g Epon 812, 2.2 g Araldite 502, 6.1 g DDSA, 0.2 g DMP-30). Some isolated spindles were prepared by the same method and others were fixed in 0.4% glutaraldehyde in PBS, pH 7.3, rinsed in PBS, fixed in 0.4% OsO_4 + 0.8% $K_3Fe(CN)_6$ in 0.1 M cacodylate buffer, pH 7.2, rinsed in cacodylate buffer for 5 min, then in distilled water three times for 5 min each, then into 2% aqueous uranyl acetate for 90 min, then dehydrated and embedded as above. Coverslips were flat-embedded on slides sprayed with release agent (MS-122; Miller-Stephenson, Sylmar, CA). After the resin had cured, coverslips were removed from the resin by dissolving them in HF for 15–20 min (31).

Spindles were mounted for sectioning in known orientation, and serial sections ~75-nm thick were picked up on slot grids. Sections were stained for 10–15 min in 1% aqueous uranyl acetate and for 5 min in lead citrate (42). Sections were viewed and photographed on a JEOL 100S electron microscope at 80 kV. Magnifications were determined from negatives of a calibration grid (cat. No. 1732, Polysciences, Inc., Warrington, PA) taken at the appropriate magnification step on the microscope.

1. *Abbreviations used in this paper*: DTT, dithiothreitol; EHNA, erythro-9-[3-(2-hydroxynonyl)]adenine.

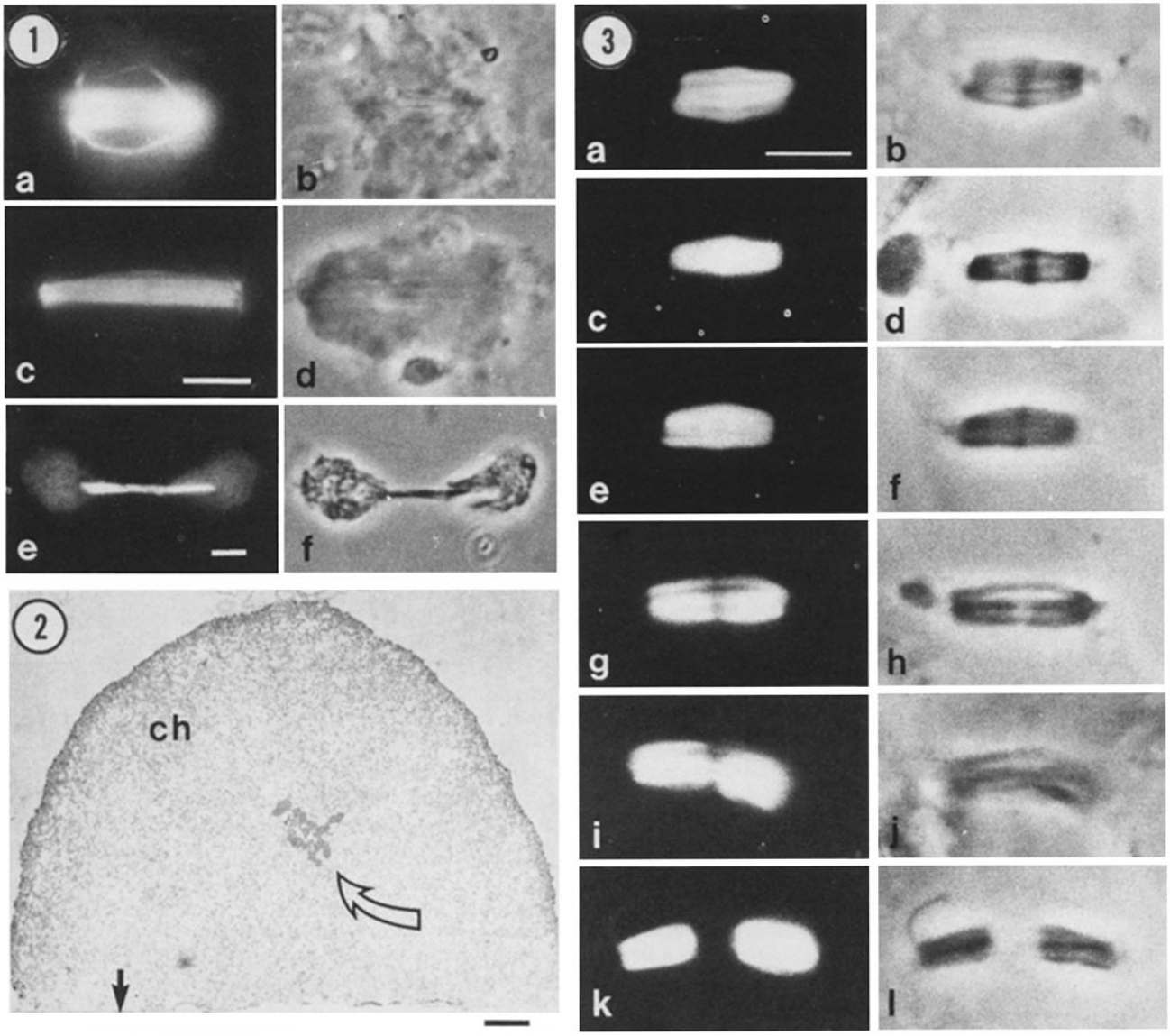

Figures 1–3. (Fig. 1) Isolated diatom spindles stained with anti-tubulin. Spindles were isolated in a pH 6.5 homogenization medium from a population of diatoms whose cell cycle was synchronized by manipulation of day length. (*a* and *b*) Phase-contrast and fluorescent micrographs of a metaphase spindle. Notice the peripheral microtubule arrays embedded in the tangled mass of chromatin. (*c* and *d*, *e* and *f*) Phase-contrast and fluorescent micrographs of an early anaphase and late anaphase spindle, respectively. Bars: (*a–f*) 5 μm. (Fig. 2) Low magnification view of a spindle in cross-section (*curved arrow*) embedded in chromatin (*ch*). The flattened portion (*arrow*) is the area where the nucleus was attached to the coverslip. Bar, 1.0 μm. (Fig. 3) (*a–l*) Isolated spindles viewed by immunofluorescence (anti-tubulin antibody) and phase microscopy after different times in 1 mM ATP. There is a prominent phase-dense and fluorescent midzone after 10 min without ATP (*a* and *b*). After 3 min in ATP (*c* and *d*) the phase-dense midzone is present to the same extent as in *a* and *b*. After 6 min in ATP (*e–h*) the phase-dense midzone is greatly reduced (*e* and *f*) or absent (*g* and *h*) and a gap begins to appear between the two half-spindles (*g* and *h*). After 10 min in ATP (*i–l*) there is large gap between the two half-spindles which is noticeable both in the phase and in the immunofluorescent image of the spindle. Bar, 5 μm.

Spindle microtubule distribution profiles were determined by counting microtubules on every fifth serial cross-section through a given central spindle on prints of ~75,000× final enlargement. A c-microtubule was identified as any microtubule that retained at least one-fourth (90° arc) of the original microtubule wall.

Results

Stephanopyxis turris has the well-ordered mitotic spindle characteristic of diatoms. Parallel arrays of microtubules extend from each pole and overlap at their distal ends to form the spindle. When stained with antibodies against tubulin after formaldehyde fixation the central spindle is a barrel-shaped structure consisting of one to several large bundles of microtubules (Fig. 1). Although the overlap zone does not usually show up as increased staining, it is, nevertheless, apparent in phase images of fixed and processed metaphase and early anaphase spindles as a distinct phase-dense region (cf. Fig. 3 *b*). It is not possible to detect the overlap zone in mid- and late-anaphase spindles. In addition, numerous peripheral microtubule bundles radiate out from the spindle poles into the chromatin mass (Fig. 1 *a*). Typically 20–30% of the spindles on a coverslip contain peripheral microtubules and none

Table I. Average Spindle Lengths of Populations of Spindles

Experiments*	*n*	% Gaps	Average spindle lengths (μm ± SD)‡		
			− ATP	+ ATP (gaps only)	+ ATP (all spindles)
1 Birefringence	25–31	85	8.4 ± 0.9	10.7 ± 0.8	10.3 ± 1.0
2 Photographs					
a	10	95	8.6 ± 0.8	10.7 ± 1.6	–
b	15	89	8.6 ± 0.7	10.1 ± 0.8	–
3 Video					
a	50	83	7.8 ± 0.7	8.7 ± 0.8	8.5 ± 0.9
b	50	90	6.1 ± 0.7	7.0 ± 0.7	6.9 ± 0.7
c	50	85	6.4 ± 0.5	7.4 ± 0.6	7.2 ± 0.6

* In Exp. 1, spindles were fixed in 0.5% glutaraldehyde and the lengths of individual spindles were measured off a TV monitor using polarization optics as described in Materials and Methods. In the two experiments in 2, individual spindles were photographed (for + ATP, gap only spindles), and measurements of spindle lengths were made from the negatives. For the experiments listed in 3, spindles were fixed in formaldehyde, processed for indirect immunofluorescence, and lengths measured off a TV monitor as described in Materials and Methods. *n*, number of spindles measured for each treatment.
‡ The difference between the means (compared with no ATP) for the experiments listed in 1 and 3 was statistically significant at $P < 0.001$ using Student's *t*-test. For the experiments listed in 2, the difference between the means (compared with no ATP) was statistically significant at $P < 0.01$ using Student's *t*-test.

are seen on the anaphase spindles. When spindles are prepared from cells that are synchronized only by the day–night cycle and not by nocodazole reversal, a variety of mitotic stages are present on the coverslips (Fig. 1). In prometaphase and metaphase spindles the chromatin has not yet reached the poles and the poles often project beyond the chromatin (Fig. 1, *a* and *b*). These spindles are typically 6–10-μm long. In early- to mid-anaphase spindles, the chromatin is more dispersed and often has reached the poles or extends beyond it (Fig. 1, *c* and *d*). In some cases the chromatin has separated into two distinct masses. These spindles are typically ~10–15-μm long. Late anaphase spindles are thin structures 15–25-μm long, and the well separated chromatin masses are found around each pole (Fig. 1, *e* and *f*). Fig. 2 shows the relationship between the spindle and the chromatin mass which is attached to the coverslip. The spindle is not always embedded in the center of the chromatin; sometimes it lies near the surface, and at later stages it is frequently near the coverslip (Fig. 2 *d* in reference 10).

In nocodazole-synchronized populations and 20 min after reversal (see Materials and Methods), the spindles are relatively uniform and are ~6–8-μm long (Figs. 3 and 5; Table I). A majority (60–80%) of these spindles are in metaphase, the rest are in early anaphase. For most of the studies described in this paper we have prepared spindles from drug-synchronized populations of cells. For most length measurements we have used only spindles that are in the same stage of mitosis, i.e., what we have defined as metaphase based on the criterion of chromatin distribution relative to the spindle poles.

Effect of ATP on Spindle Structure and Length

Addition of 1 mM ATP leads to striking structural changes in the central spindle (Figs. 3–11) and these changes occur in >75% of the spindles under normal reactivation conditions (Table I). When viewed by polarization optics (10) or by indirect immunofluorescence with tubulin antibodies, the two half-spindles have become separated and the spindle midzone is bridged by only a few microtubules. The phase-dense material that delineates the microtubule overlap zone is progressively lost over time and is not present in spindles that display gaps between the half-spindle (Fig. 3, *e* and *f* vs. *g* and *h*). Peripheral microtubules are also absent after ATP treatment and the percentage of spindles with peripheral microtubules is reduced from 28% to 2% after a 3-min exposure to ATP.

An increase in average spindle length precedes or accompanies the structural changes that occur in ATP (Fig. 4). The difference in average spindle length is statistically significant when compared with untreated spindles regardless of whether all ATP-treated spindles or only structurally altered spindles with gaps are used for the length comparison (Table I). The length changes measured range from 12 to 27% of the original spindle length and this is about equivalent to one times the size of the original microtubule overlap zone. As is shown by comparing the spindle length histograms in Fig. 5, the smallest spindles in the ATP-treated populations are usually those that have unaltered microtubule overlap zones.

At the electron microscope level, the changes in spindle structure caused by ATP are most readily seen as fewer microtubules and decreased packing order in the zone of overlap (Figs. 6–7). Fig. 6 is a cross-section through the overlap region of a metaphase cell in vivo. There are over

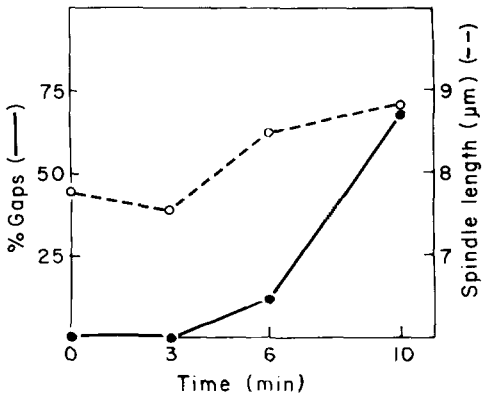

Figure 4. The response of isolated spindles to addition of ATP over time. This is the same experiment shown in Fig. 3. 100 spindles per time point were scored for gaps (●) and 50 metaphase spindles were measured for length change (○). The difference between means (compared with no ATP) for the 6- and 10-min spindle length determinations was statistically significant at $P < 0.001$ using Student's *t*-test.

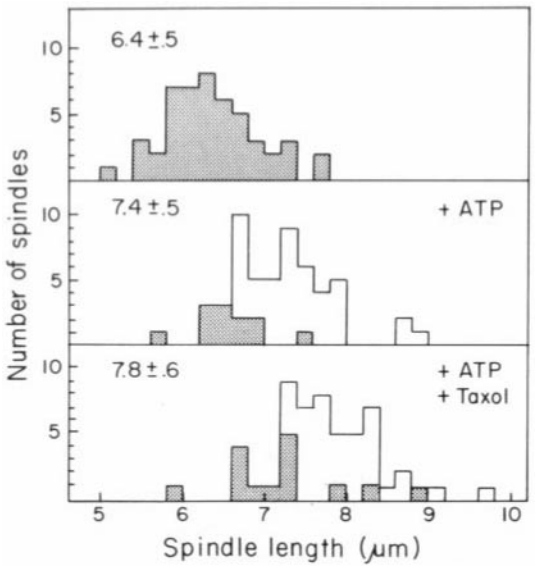

Figure 5. Histograms of the lengths of spindles after 10 min in a variety of incubation conditions. Spindles with prominent microtubule overlap zones are shown as shaded areas while those with midzone structural alterations (gaps) are not shaded in. Average spindle length (±SD) is given in the upper left-hand corner of each panel. *Top*, no ATP; *middle*, 1 mM ATP; *bottom*, 1 mM ATP and 10 μM taxol. See also Table III.

600 closely packed microtubules enmeshed in an osmiophilic matrix material. A cross-section through the same region of an isolated spindle in medium without ATP (Fig. 2 *c* in reference 10) shows an equivalent number of closely packed microtubules though the chromatin and osmiophilic matrix material have become dispersed. However, if ATP is added then the structure of the spindle is dramatically altered within 5 min (Fig. 7) and by 10 min only a fraction of the microtubules, if any, are left in the overlap (cf. Fig. 2 *d* in reference 10). There is relatively little, if any, osmiophilic material in the overlap zone of this spindle which has elongated in vitro.

We have examined the effects of ATP on isolated central spindle microtubules by serial cross-section analysis of spindles after 0, 1, 5, and 10 min in reactivation medium. Microtubule distribution profiles (microtubule number vs. position along the spindle long axis) were prepared for each time point by counting total microtubules and c-microtubules on every fifth section (Figs. 8–11). We find that microtubules are lost first from the zone of overlap and then throughout each half-spindle. The increase in c-microtubule profiles corresponds to regions of microtubule loss. In isolated spindles minus ATP (Fig. 8) each half-spindle has ~300 microtubules and 600 microtubules in the overlap zone, and c-microtubule profiles are distributed more or less evenly

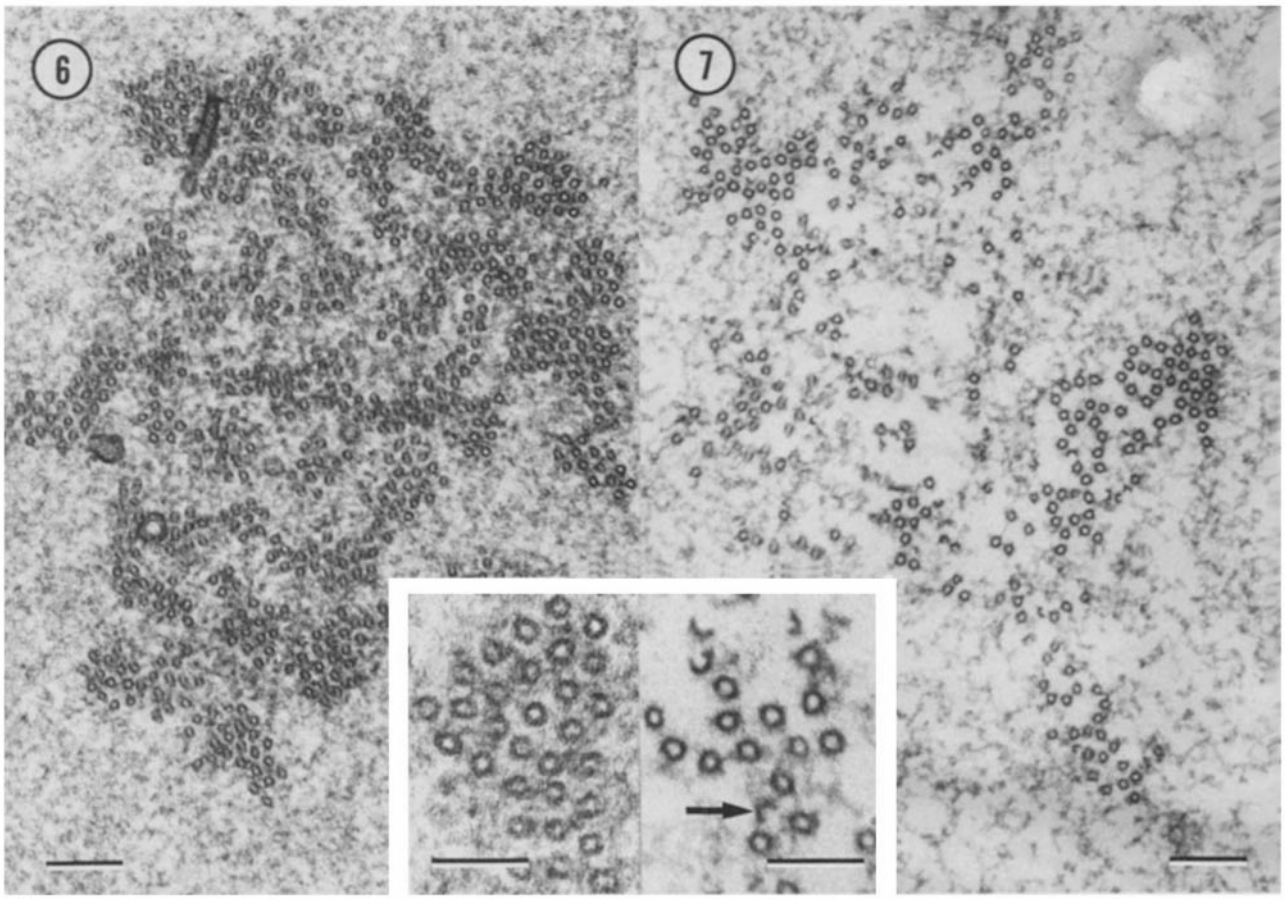

Figures 6 and 7. (Fig. 6) Cross-section through the overlap region of a metaphase central spindle in vivo. Osmiophilic material (*inset*) is distributed among the microtubules. Bar, 0.2 μm. (*Inset*) Bar, 0.1 μm. (Fig. 7) Cross-section through the overlap region of a central spindle after 5 min in reactivation medium containing ATP. The orderly arrangement of microtubules (compare with Fig. 6) has been disrupted and c-microtubule profiles (*arrow* in *inset*) are more apparent. Bar, 0.2 μm. (*Inset*) Bar, 0.1 μm.

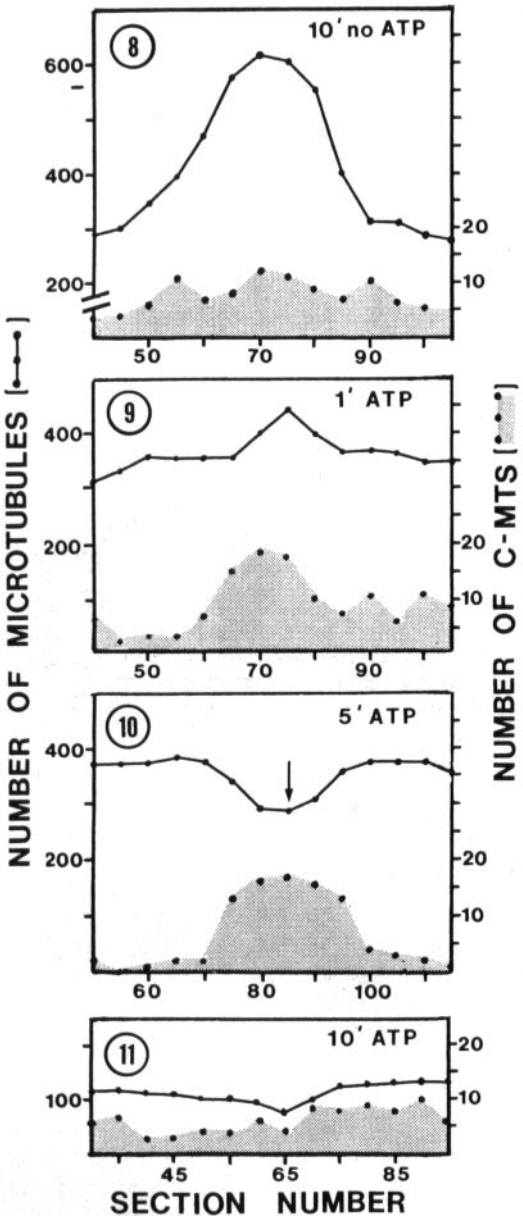

Figures 8–11. Microtubule distribution profiles through the overlap regions of an isolated metaphase spindle without added ATP (Fig. 8), an isolated spindle after 1 min in ATP (Fig. 9), 5 min in ATP (Fig. 10), and 10 min in ATP (Fig. 11). C-microtubule distribution profiles (shaded areas) are shown for each spindle. The arrow in Fig. 10 indicates the position of the section shown in Fig. 7.

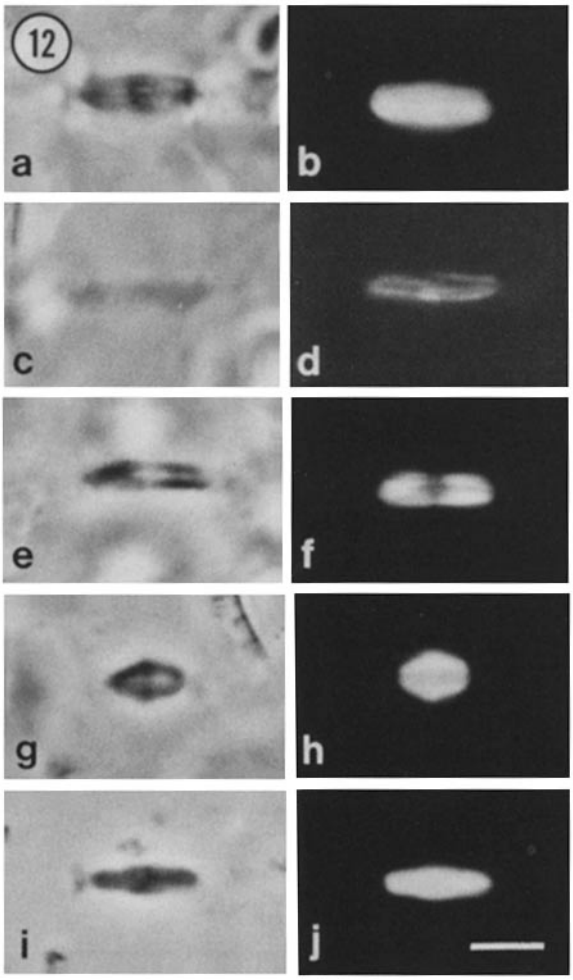

Figure 12. Phase and fluorescent micrographs of spindles after various treatments to demonstrate the lability properties of isolated spindles in the absence of ATP. In *a–d* spindles were incubated in pH 7.0 medium for 10 min (*a* and *b*) and 3 h (*c* and *d*) at room temperature. After 3 h there is extensive microtubule depolymerization and the phase-dense midzone is greatly reduced. In *e* and *f* the spindle was incubated for 3 h at room temperature in 5 μM taxol and the extent of microtubule depolymerization has decreased compared with *c* and *d*. In *g* and *h* spindles were incubated for 10 min in 10 mM sodium tetrapyrophosphate and (*i* and *j*) in 2 M potassium acetate. In pyrophosphate spindles decreased 20–30% in length; however, after either treatment the overlap zone was still persistent. Bar, 5 μm.

across this region. However, even after 1 min in ATP the microtubules are actively depolymerizing as shown by the reduced height of the overlap peak (but not the half-spindle) and the relative increase in c-microtubule profiles in the spindle midzone (Fig. 9). After 5 min in ATP (Fig. 10) the half-spindle microtubule numbers are still ~300 but controlled disassembly of microtubules in the midzone is now revealed by a dip in the curve at that point. The c-microtubule number is still high in the spindle midregion. By 10 min microtubule numbers are reduced throughout the spindle and c-microtubule profiles more uniformly distributed (Fig. 11).

Lability of Isolated Spindle Microtubules

We have begun to explore the effects of various treatments on spindle structure and we report here a few treatments that demonstrate the lability of the spindle microtubules in the absence of ATP (Fig. 12). We find that overall spindle structure is affected by the pH of the homogenization and incubation medium. Spindles prepared at pH 6.5 (Fig. 1) are slightly longer and more compact than spindles prepared at pH 7.0 (Figs. 3, 12, and 13) and their microtubules are more resistant to exposure to high salt. In the absence of glycerol, at pH 7.0 and room temperature (20°C) central spindle microtubules slowly depolymerize. After 10 min (Fig. 12, *a* and *b*, and unpublished data) peripheral microtubules are

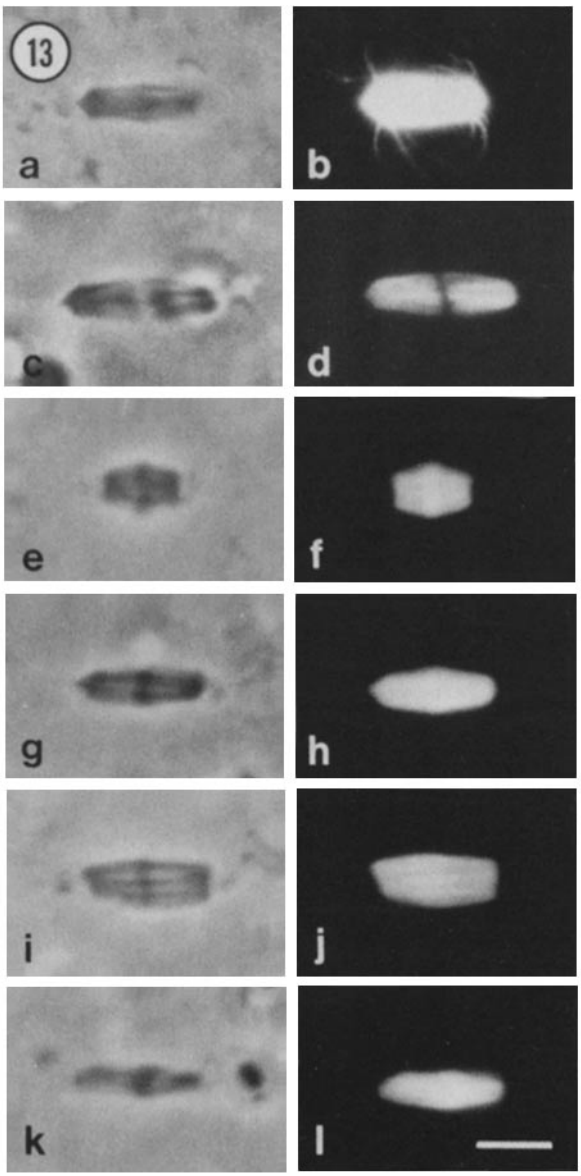

Figure 13. Phase and fluorescent micrographs of the same spindle after different treatments to show the effects of various nucleotides and inhibitors on spindle reactivation. In *a* and *b* spindles were incubated in 1 mM CTP for 10 min. In *c* and *d* spindles were incubated in 1 mM ATP and 10 μM taxol for 10 min. In *e* and *f* spindles were incubated in 0.5 mM ATP and 2.5 mM AMPPNP. These spindles retain their overlap zone but are shorter than similar spindles incubated in the absence of nucleotides or in AMPPNP alone. In *g* and *h* spindles were incubated for 3 min in 1 mM ATP, then washed and transferred to a medium containing 1 mM AMPPNP for 10 min. Spindle reactivation ceased after transfer to AMPPNP. In *i* and *j* spindles were incubated for 10 min in 1 mM ATP and 100 μM vanadate. No spindle elongation has occurred; however, the peripheral microtubules arrays are gone. In *k* and *l* spindles were incubated for 3 min in 1 mM ATP, then 100 μM vanadate was added with vigorous stirring and spindles were incubated for an additional 10 min. No spindle elongation occurred. Bar, 5 μm.

still present and the central spindle is not noticeably different from those spindles fixed immediately after removal from glycerol. However, after 3 h, the spindles display greatly reduced overall fluorescence and loss of phase-dense material

Table II. Nucleotide Requirements for Spindle Reactivation

Nucleotide (1 mM)	% Gaps*
0	0
ATP	82
ADP, CTP, GTP, ITP, UTP	0
ATPγS, deoxyATP, AMPPNP	0
ATP + ATPγS	63
ATP + AMPPNP	0

* Approximately 100–150 spindles were scored for each experimental treatment. Coverslips were incubated for 10 min in nucleotide before fixation.

and microtubules from the overlap zone (Fig. 12, *c* and *d*). These changes can be retarded but not completely blocked by 5 μM taxol (Fig. 12, *e* and *f*), and these changes are accelerated by incubation in medium at pH 7.5 or pH 8.0 (unpublished data). Spindles can be stored on ice in 30% glycerol for 2 d without an apparent loss of microtubules and after ATP addition 10–30% of these spindles still undergo spindle reactivation. Brief exposure to 10 mM sodium tetrapyrophosphate (Fig. 12, *g* and *h*) or high salt (Fig. 12, *i* and *j*) leads to a slight overall reduction in immunofluorescence and, in the presence of sodium tetrapyrophosphate, a one-third reduction in overall spindle length. Significantly, neither treatment induces loss of phase-dense midzone material and the formation of gaps between the half-spindles. Peripheral microtubules are the most labile part of the spindle and are not retained after any of these treatments. Isolated spindles are not affected by 10-min exposure to nocodazole even though micromolar nocodazole blocks spindle formation in vivo (56). Other drugs such as erythro-9-[3-(2-hydroxynonyl)]adenine (EHNA), cytochalasin B, and phalloidin also do not affect spindle structure during a 10-min incubation at room temperature.

Nucleotide Requirement for Spindle Elongation In Vitro

To determine whether ATP hydrolysis was required for reactivation of spindle elongation and related events, nonhydrolyzable ATP analogues were substituted for ATP. As shown in Table II and Fig. 13, neither ATPγS, AMPPNP, nor deoxyATP will support midzone structural changes and reactivation of spindle elongation. In addition, AMPPNP, when added in equimolar ratios with ATP, blocks spindle elongation and gap formation (Table II, Fig. 13, *e* and *f*). These spindles also have an unusual morphology. They are distinctly shorter than spindles treated with AMPPNP only or no nucleotide. This effect is not seen with the addition of ATPγS and ATP.

Reactivation of spindle elongation is highly specific for ATP (Table II; Fig. 5, *a* and *b*) and no other nucleotide supports this process (cf. Fig. 13, *a* and *b*). In preliminary experiments GTP generated some (10%) gaps but these effects were eliminated by including in the incubation medium an enzyme (hexokinase and glucose) that uses ATP as a substrate. This suggests that the GTP was contaminated by low levels of ATP or that a kinase that can convert GTP to ATP was present in the spindle preparations.

Peripheral microtubule loss also requires ATP hydrolysis (unpublished data) and displays a nucleotide specificity simi-

lar to that required for reactivation of spindle elongation. Although we have not attempted to quantify this, nonhydrolyzable analogues do not apparently diminish the number of spindles containing peripheral microtubules.

To determine whether continuous ATP hydrolysis is required for spindle reactivation we have removed spindles from ATP after 3-min incubations (before significant spindle elongation and gap formation have occurred; see Fig. 4) and placed them in AMPPNP or a medium without ATP. After transfer to either of these media no spindle reactivation occurs (Fig. 13, *g* and *h*) and the spindles look similar to those incubated continuously in a medium without nucleotide except for the loss of peripheral microtubules. A similar response is observed with addition of vanadate to the incubation medium after 3 min in ATP (Fig. 13, *k* and *l*).

Using an ATP-regenerating system to buffer ATP concentrations at different levels, we have examined the dependence of spindle midzone structural changes on nucleotide concentration (Fig. 14). The maximum number of reactivated spindles are seen in 1 mM ATP although at 100 μM ATP the percentage of reactivated spindles is ~2/3 that seen at the higher ATP concentrations (Fig. 14 *a*). Below 25 μM ATP no distinct gaps are seen although in some spindles the midzones appear to be faded. Between 25 and 100 μM ATP the number of gaps between half-spindles increases, but these are less pronounced than at higher ATP concentrations. The response of spindles to different ATP concentrations depends on the stage of mitosis. As shown in Fig. 14 *b*, most of the gaps seen in 25–50 μM ATP are found in spindles that are derived from cells that were in early anaphase, not metaphase, at the time of isolation (Fig. 14 *b*). In one experiment, we measured from photographs the lengths of 10–20 reactivated spindles per nucleotide concentration after 10-min exposure to 100 μM, 0.5 mM, and 1 mM ATP. These spindles on the average were longer than those that had not seen ATP, and no differences in length could be detected between the different populations of spindles (Table I, Exp. 2a and data not shown).

Inhibitor Studies

Isolated spindles were reactivated in a variety of drugs known to interfere with actomyosin or microtubule-based motility in a variety of cell types (Table III). It is not known whether EHNA interferes with cytoskeletal function in vivo in diatoms; however, at the concentrations used here we have found that nocodazole blocks spindle formation in vivo (56) and cytochalasin blocks cytokinesis but not mitosis in other diatoms (47). With the exception of taxol, vanadate, and sulfhydryl reagents, none of these drugs affected spindle elongation or the appearance of gaps in vitro (Table III).

Taxol stabilizes microtubules in many cell types, including plants (32) and *Poterioochromonas*, a close relative to the diatoms (18), and it retards central spindle microtubule depolymerization (Fig. 12, *e* and *f*). As shown by comparing spindle length distribution histograms (Fig. 5), isolated diatom spindles incubated in taxol elongate more than comparable spindles incubated in ATP alone; however, both classes of spindles show similar midzone structural rearrangements and gaps between the two half-spindles (Table III, Fig. 13, *c* and *d*). The extent of spindle elongation was 0.8 μm in ATP and 1.4 μm in ATP plus taxol. This represents a 15% increase in average spindle lengths for ATP-treated spindles and a 25% increase over original (minus ATP) spindle length for spindles incubated in taxol and ATP (Table III, Fig. 5).

Vanadate, an inhibitor of dynein ATPase activity in cilia and flagella (15) and of anaphase B in permeabilized PtK_1 cells (8, 12), inhibited spindle reactivation when added with ATP or when added after several minutes in ATP (Fig. 13). In the absence of DTT and at low ATP concentrations, complete inhibition of spindle reactivation is achieved with 25 μM vanadate and 95% inhibition with 10 μM vanadate (Fig. 15, Table III). Concentrations ≤5 μM are noninhibitory (Fig. 15). Vanadate inhibition of spindle reactivation could be reversed by washing out the vanadate although reversal is not complete (Table III). Peripheral microtubule loss due to ATP is vanadate-insensitive; it occurs in the presence of vanadate even if added together with ATP. For example, after 2 min in ATP with or without vanadate only 5% of the spindles retained peripheral microtubules.

Salygrin and N-ethylmaleimide, sulfhydryl reagents that inhibited anaphase B in lysed PtK_1 cells (8), also block reactivation of spindle elongation in isolated diatom spindles (Table III). This is consistent with our observation that preparation of isolated spindles capable of subsequent reactivation is greatly aided by inclusion of DTT in the homogenization and reactivation medium. For example, in the experiments shown in Fig. 15 no DTT was included in the reactivation medium and the level of spindle reactivation,

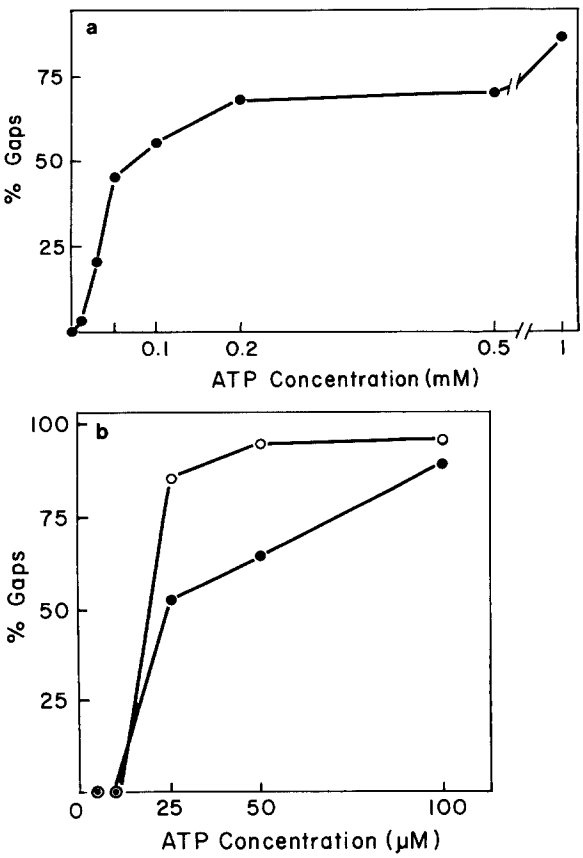

Figure 14. The response of isolated spindles to ATP as a function of ATP concentration. (*a*) 100 spindles were scored for each ATP concentration regardless of mitotic stage. (*b*) ●, the response of metaphase spindles; ○, the response of anaphase spindles to different ATP concentrations. In this experiment (*b*) 30% of spindles were in early anaphase and 70% of the spindles in metaphase.

Table III. The Effect of Inhibitors of Cytoskeletal Function on Spindle Elongation and Gap Formation In Vitro

Treatment*	% Gaps	Average spindle lengths‡
		μm ± SD
Controls		
0 ATP	0	6.4 ± 0.5
1 mM ATP	85	7.4 ± 0.5§
Actomyosin inhibitors		
10 μM Cytochalasin D	74	7.6 ± 0.8§
70 μg/ml Phalloidin	81	–
Microtubule inhibitors		
10^{-6} M Nocodazole	73	–
10 M Taxol	70	7.8 ± 0.6§‖
2 mM EHNA (+ 0.25 mM ATP)	90	7.5 ± 0.8§
Vanadate		
10 μM Vanadate (+ 100 μM ATP)	2	–
100 μM Vanadate (+ 1 mM ATP)	0	6.3 ± 0.5
10 μM Vanadate (3 min), then 1 mM ATP (10 min)	50	–
100 μM Vanadate (3 min), then 1 mM ATP (10 min)	13	–
Sulfhydryl reagents		
10^{-5} M Salygrin	0	–
10^{-5} N-Ethylmaleimide	33	–

* Coverslips were incubated for 10 min in the presence of the drug and with 1 mM ATP unless otherwise indicated. No effects of these treatments were observed in the absence of ATP.
‡ At least 50 metaphase spindles were measured for all length determinations and 100 spindles scored for all gap determinations. No length measurements were made for several of the treatments.
§ The difference between the means (compared with no ATP) was statistically significant at $P < 0.001$ using Student's *t*-test.
‖ The difference between the means (compared with 1 mM ATP) was statistically significant at $P < 0.005$ using Student's *t*-test.

even in the absence of any drug treatment, was considerably less than that observed in other experiments.

Discussion

Spindle Reactivation in Vitro

The response of the isolated diatom spindle to ATP addition is complex and mimics many aspects of in vivo anaphase.

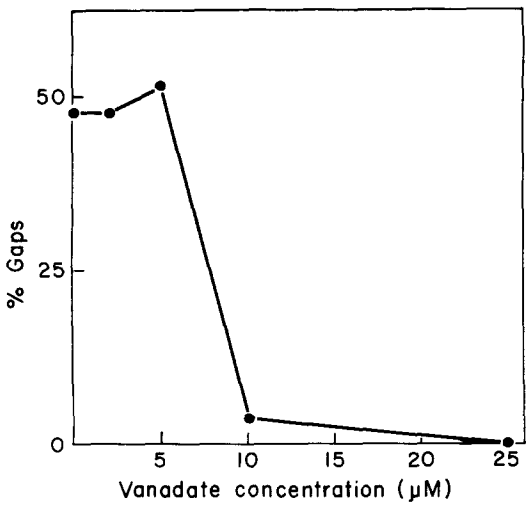

Figure 15. Effect of vanadate on spindle reactivation. Spindles were incubated for 10 min at room temperature at different vanadate concentrations in 100 μM ATP and without DTT present.

Time-lapse video studies (10) and the experiments described here suggest that spindle elongation in vitro includes three classes of ATP-dependent events: (*a*) initiation, (*b*) separation of the half-spindles, and (*c*) selective microtubule depolymerization from the overlap zone poleward. As shown by polarization optics or indirect immunofluorescence, almost all of the spindles in our preparations undergo this complex behavior. The successful development of isolated spindle preparations that reproducibly and uniformly undergo spindle elongation in vitro means that it will now be possible to biochemically dissect this process and to analyze it ultrastructurally with some assurance that the machinery responsible for anaphase B is present in a typical form and a functional state.

The extent of spindle elongation in vitro is only 12–27% (Tables I and III) but this is exactly what we would predict if the half-spindles slide apart due to mechanochemical interactions in the zone of microtubule overlap. The length of the microtubule overlap, which is 15–25% of the original spindle length (10), will determine the maximum extent of elongation observed in vitro (i.e., one times the overlap) if the microtubules of one half-spindle use the microtubules of the other half-spindle as the substrate for mechanochemical activity. If elongation were due to nonspecific causes such as chromatin swelling or to the autonomous "swimming" apart of the half-spindles we would expect at least some of the spindles to elongate more than the extent of the overlap zone, but none do. Spindle elongation in vitro would also be affected by the stability of microtubules in each half-spindle. Addition of taxol retards the ATP-induced lability of central spindle microtubules, and these spindles elongate more than spin-

dles incubated in ATP only (Fig. 5). Treatments that accelerate diatom microtubule depolymerization, such as incubation in high pH (7.5–8.0) decrease the extent of spindle elongation in vitro (Cande, W. Z., and H. Masuda, unpublished data). Finally we predict that if isolated spindles could incorporate tubulin and use it to support spindle function, they would not be restricted in the extent of elongation observed in vitro. In preliminary experiments after the incorporation of neurotubulin into diatom spindles we find that some isolated spindles elongate severalfold more than the original overlap zone length (Masuda, H., and W. Z. Cande, unpublished data).

Initiation

The kinetics of spindle reactivation have led us to postulate a set of unique ATP-dependent regulatory events that are required before spindle elongation and central spindle microtubule depolymerization can commence. From perfusion studies monitored by time-lapse video, we know that spindle elongation does not commence until several minutes after ATP addition (10). A similar lag before elongation begins is observed with populations of spindles (Fig. 4). Although peripheral microtubule bundles disappear within 3 min after ATP addition, central spindle microtubule depolymerization occurs more slowly and, unlike peripheral microtubule loss, can be blocked by vanadate. Initiation events may be mitotic stage–dependent since anaphase and metaphase spindles differ in their minimal ATP concentration requirements for reactivation. A regulatory phosphorylation cascade is a logical candidate for these initiation events. The spindle contains many phosphorylated structures (54), and we have shown that isolation of spindles in conditions favoring endogenous acid phosphatase activity substantially inhibits subsequent ATP-dependent spindle reactivation (55). Moreover, addition of 40 mM Na glycerophosphate or 50 μM ATPγS, treatments that block phosphatase activity, greatly increases the percentage of reactivated spindles and the rates at which they elongate.

Spindle Mechanochemistry

The process of spindle elongation that we observe in vitro is consistent with models of force generation which postulate that mechanochemical interactions in the zone of microtubule overlap play a major role in generating the forces required for spindle elongation (27–30). Our results can best be interpreted by imagining that the microtubules of one half-spindle push off against the microtubules of the other half-spindle, generating sliding forces between them. Using ultraviolet (UV) microbeaming, Leslie and Pickett-Heaps (24) have demonstrated that anaphase B in living diatoms also depends on the generation of sliding forces in the zone of microtubule overlap. The forces responsible for spindle elongation in vitro could not have been generated by microtubule polymerization (20) since no tubulin is present during reactivation. Similarly, the half-spindles could not have been pulled apart by forces generated in the cytoplasm (3, 23) since no cytoplasmic structures are attached to the spindle poles in vitro (10). Although it has been suggested that chromatin swelling during reactivation could pull the half-spindles apart we think that this possibility is also unlikely. Spindle elongation and gap formation can be observed with central spindles whose chromatin has been removed by DNAse digestion or whose chromosomes have been stabilized by addition of spermidine and spermine (McDonald, K., K. Pfister, H. Masuda, L. Wordeman, C. Staiger, and W. Z. Cande, manuscript in preparation).

In the past we have argued for the involvement of a dynein-like ATPase in spindle elongation and have emphasized the similarities between reactivated flagellar models and spindle elongation in vitro, especially with respect to nucleotide specificity, vanadate inhibition, and sulfhydryl reagent sensitivity (8, 11, 12). Recently, Vale et al. (51) have described another ATPase, kinesin, which may be responsible for the anterograde movement of organelles over cytoplasmic microtubules during fast axonal transport. The nucleotide specificity of spindle elongation in vitro and its inhibition by nonhydrolyzable nucleotide analogues is consistent with the involvement of either dynein (11, 36) or kinesin (51), but not myosinlike ATPases (1, 41), in this process. Since AMPPNP in the presence of ATP can block spindle elongation, this suggests that a motor with a kinesinlike cross-bridge cycle may be involved in anaphase B (51). However, kinesin ATPase activity is insensitive to sulfhydryl reagents, whereas both reactivated flagellar beat and spindle elongation in vitro are inhibited by sulfhydryl reagents, such as salygrin and N-ethylmaleimide (1, 6). Moreover, flagellar beat (15) and spindle elongation in vitro are completely blocked by vanadate concentrations that have no effect on kinesin-based movement (51). However, since flagellar dynein has a relatively low affinity for AMPPNP, it may not be a good candidate for the spindle motor. We therefore argue that the ATPase responsible for the pushing apart of microtubules of opposite polarity during spindle elongation may either be a dyneinlike molecule with some unique properties or a new and as yet undescribed microtubule-based mechanochemical enzyme. With reference to pharmacology, it is similar to the retrograde particle transport motor that is present in crude extracts of squid axon (52).

Since the physiological requirements for spindle elongation in lysed mammalian cells and diatom spindles are similar (8, 11, 12), an analogous mechanism may be important for anaphase B in a wide variety of cells. Most of the differences observed between these two systems for maintaining anaphase B, such as the minimal ATP concentration required for movement, are minor and may have more to do with the complexity of the lysed cell vs. the relative simplicity of the isolated diatom spindle. However, anaphase B in lysed PtK_1 cells is inhibited by EHNA (9), a weak but specific dynein ATPase inhibitor (7), but under identical incubation conditions EHNA did not affect spindle elongation in isolated diatom spindles. We have no explanation for this difference other than to suggest that the target ATPases in mammalian and diatom spindles may differ in sensitivity to EHNA. It has not been reported whether EHNA blocks dynein ATPase activity in cilia derived from algae or protozoa. Also, the specificity of EHNA as a dynein inhibitor is now suspect since Schliwa et al. (46) have shown that it interferes with actomyosin-based motility in several cell types.

ATP-induced Specific Microtubule Depolymerization

The ATP-induced microtubule length changes and the mechanochemical events leading to spindle elongation in vitro and in vivo must be closely coupled processes. Nor-

mally, in this diatom and in many other cells microtubule growth is an integral part of anaphase B and leads to an increase in spindle length much greater than can be generated by microtubule rearrangement alone. In *S. turris*, the late anaphase spindle is several times longer than the metaphase spindle and only a fraction of this length increase could occur in the absence of microtubule growth (56; and McDonald, K., K. Pfister, H. Masuda, L. Wordeman, C. Staiger, and W. Z. Cande, manuscript in preparation). It is clear, at least in *S. turris*, that sliding and microtubule length changes occur at the same time and are not sequential events, as claimed by Tippit et al. for the rust fungus *Puccinia* (50). Tubulin subunit addition presumably occurs at the plus (or assembly-favored) ends, which are clustered together in the zone of microtubule overlap (14, 48). To explain the in vivo behavior of spindles during elongation, the rate of subunit addition must be coupled to or regulated by the rate by which the half-spindles slide apart. Margolis et al. (27) have suggested that microtubule treadmilling could provide such a mechanism although the lability properties of diatom spindle microtubules in vivo (25, 40, 47) and in vitro are inconsistent with this hypothesis.

The defined pattern of microtubule depolymerization that accompanies spindle elongation in vitro may be an expression of the mechanism that links microtubule length change to microtubule sliding. In the absence of a tubulin subunit pool, central spindle microtubules depolymerize from the overlap zone poleward rather than grow. Microtubule depolymerization may depend on the rate of spindle elongation in vitro since there is no obvious decrease in half-spindle birefringence (10; unpublished data) or generation of a gap between the half-spindles until spindle elongation is almost completed (cf. Fig. 4). Under identical incubation conditions, the peripheral microtubule bundles disappear rapidly and before spindle elongation has begun. For both classes of microtubules, there may be a discrete cap on the plus end of every microtubule equivalent to stop proteins (26) or MAP2 (53) that regulates microtubule assembly-disassembly in an ATP-dependent manner. In addition, in the central spindle lateral interactions between overlapping microtubules may help stabilize them, and as the two half-spindles separate giving less overlap, the microtubules begin to depolymerize.

We have some assurance that the ATP-dependent microtubule depolymerization we observe in vitro is not an artifact of spindle isolation since a similar process occurs during telophase in the diatom *Pinnularia* (47) and after UV microbeaming of diatom spindles (25). Controlled microtubule length changes are an important part of mitosis in all cells, since prometaphase chromosome movements, chromosome to pole movements during anaphase A, and spindle elongation during anaphase B require that kinetochore or polar microtubules shorten or lengthen (19). Although there is ample precedent for ATP-dependent changes in microtubule lability from both in vitro (21, 22, 26, 33, 53, 57) and in vivo (4, 5, 13, 37) studies, the mechanism by which ATP induces these changes is not well understood. Since we have recently found that isolated diatom spindles can incorporate exogenous tubulin and use these new microtubules to support further spindle elongation (Masuda, H., and W. Cande, unpublished observations), isolated diatom spindles may thus prove to be a useful starting point for understanding how cells regulate microtubule lengths in a coordinate fashion.

We thank Dan Coltrin, Ellen Dean, and Douglas Ohm for technical assistance, Dr. Benjamin Volcani for advice on growing diatoms, and Dr. Kevin Pfister and Linda Wordeman for help in interpreting these experiments.

This work was supported by National Institutes of Health grant GM-23238 and National Science Foundation grant PCM-8408594.

Received for publication 6 November 1985, and in revised form 25 March 1986.

References

1. Arronet, N. I. 1973. Motile Muscle and Cell Models. B. Haigh, translator. Plenum Publishing Corp., New York. 1–192.

2. Asai, D. J., C. J. Brokaw, W. C. Thompson, and L. Wilson. 1982. Two different monoclonal antibodies to α tubulin inhibit the bending of reactivated sea urchin spermatozoa. *Cell Motil.* 2:599–614.

3. Bajer, A. S. 1982. Functional autonomy of monopolar spindles and evidence for oscillatory movements in mitosis. *J. Cell Biol.* 93:33–48.

4. Bershodsky, A. D., and V. I. Gelfand. 1981. ATP-dependent regulation of cytoplasmic microtubules disassembly. *Proc. Natl. Acad. Sci. USA.* 78: 3610–3613.

5. Bershodsky, A. D., and V. I. Gelfand. 1983. Role of ATP in the regulation of the stability of cytoskeletal structures. *Cell Biol. Int. Rep.* 7:173–187.

6. Blum, J. J., and A. Haynes. 1978. Effect of sulfhydryl reagents on the ATPase activity of solubilized 14S and 30S dyneins and on whole ciliary axonemes as a function of pH. *J. Supramol. Struct.* 8:153–171.

7. Bouchard, P., A. Cheung, S. Penningroth, C. Gagnon, and C. Bardin. 1981. Erythro-9-[3-(2-hydroxy-3-nonyl)]adenine is an inhibitor of sperm motility that blocks dynein ATPase and protein carboxymethylase activities. *Proc. Natl. Acad. Sci. USA.* 78:1033–1036.

8. Cande, W. Z. 1982. Nucleotide requirements for anaphase chromosome movements in permeabilized mitotic cells: anaphase B but not A requires ATP. *Cell.* 28:15–22.

9. Cande, W. Z. 1982. Inhibition of spindle elongation in permeabilized mitotic cells by erythro-9-[3-(2-hydroxynonyl)]adenine. *Nature (Lond.).* 295: 700–701.

10. Cande, W. Z., and K. L. McDonald. 1985. In vitro reactivation of anaphase spindle elongation using isolated diatom spindles. *Nature (Lond.).* 316:168–170.

11. Cande, W. Z., K. McDonald, and R. L. Meeusen. 1981. A permeabilized cell model for studying cell division: a comparison of anaphase chromosome movement and cleavage furrow constriction in lysed PtK_1 cells. *J. Cell. Biol.* 88:618–629.

12. Cande, W. Z., and S. M. Wolniak. 1978. Chromosome movement in lysed mitotic cells is inhibited by vanadate. *J. Cell Biol.* 79:573–580.

13. DeBrabander, M., G. Guens, R. Nuydens, R. Willebrods, and J. DeMey. 1982. Microtubule stability and assembly in living cells: the influence of metabolic inhibitors, taxol and pH. *Cold Spring Harbor Symp. Quant. Biol.* 46:227–239.

14. Euteneuer, U., and J. R. McIntosh. 1980. The polarity of midbody and phragmoplast microtubules. *J. Cell Biol.* 87:509–515.

15. Gibbons, I. R., M. P. Cosson, J. A. Evans, B. H. Gibbons, B. Houck, K. H. Martinson, W. S. Sale, and W.-J.Y. Wang. 1978. Potent inhibition of dynein adenosine triphosphatase and the motility of cilia and flagella by vanadate. *Proc. Natl. Acad. Sci. USA.* 75:2220–2224.

16. Goode, D., and L. E. Roth. 1965. The mitotic apparatus of a giant amoeba: solubility properties and induction of elongation. *Exp. Cell Res.* 58:343–352.

17. Guillard, R. R. L. 1975. Culture of phytoplankton for feeding marine invertebrates. *In* Culture of Marine Invertebrate Animals. W. Smith and H. Chanley, editors. Academic Press, Inc., New York. 21–88.

18. Herth, W. 1983. Taxol effects cytoskeletal microtubules, flagella and spindle structure of the Chrysoflagellate alga *Poterioochromonas. Protoplasma.* 115:228–239.

19. Inoué, S. 1981. Cell division and the mitotic spindle. *J. Cell Biol.* 91(3, Pt. 2):131s–147s.

20. Inoué, S., and H. Sato. 1967. Cell motility by labile association of molecules. *J. Gen. Physiol.* 50(Suppl.):259–292.

21. Jameson, L., and M. Caplow. 1981. Modification of microtubule steady-state dynamics by phosphorylation of the microtubule-associated proteins. *Proc. Natl. Acad. Sci. USA.* 78:3413–3417.

22. Jameson, L., T. Frey, B. Zeeberg, F. Calldorf, and M. Caplow. 1980. Inhibition of microtubule assembly by phosphorylation of microtubule-associated proteins. *Biochemistry.* 19:2472–2479.

23. Kronebusch, P. J., and G. G. Borisy. 1982. Mechanics of anaphase B movement. *In* Biological Functions of Microtubules and Related Structures. H. S. Sakai and G. G. Borisy, editors. Academic Press, Inc., New York. 233–245.

24. Leslie, R. J., and J. D. Pickett-Heaps. 1983. Ultraviolet microbeam irradiations of mitotic diatoms: investigation of spindle elongation. *J. Cell Biol.* 96:548–561.

25. Leslie, R. J., and J. D. Pickett-Heaps. 1984. Spindle microtubule dynamics following ultraviolet-microbeaming irradiations of mitotic diatoms. *Cell.* 36:717–727.

26. Margolis, R. L., and C. T. Rauch. 1981. Characterization of rat brain crude extract microtubule assembly: correlation of cold stability with the phosphorylation state of a microtubule-associated 64K protein. *Biochemistry.* 20:4451–4458.

27. Margolis, R. L., L. Wilson, and B. I. Kiefer. 1978. Mitotic mechanism based on intrinsic microtubule behavior. *Nature (Lond.).* 272:450–452.

28. McDonald, K. L., M. K. Edwards, and J. R. McIntosh. 1979. Cross-sectional structure of the central mitotic spindle of *Diatoma vulgare*. *J. Cell Biol.* 83:443–461.

29. McDonald, K. L., J. D. Pickett-Heaps, J. R. McIntosh, and D. H. Tippit. 1977. On the mechanism of anaphase spindle elongation in *Diatoma vulgare*. *J. Cell Biol.* 74:377–388.

30. McIntosh, J. R., P. K. Hepler, and D. G. Van Wie. 1969. Model for mitosis. *Nature (Lond.).* 224:659–663.

31. Moore, M. J. 1975. Removal of glass coverslips from cultures flat embedded in epoxy resin using hydrofluoric acid. *J. Microsc.* 104:205–207.

32. Morejohn, L. C., and D. E. Foshet. 1984. Taxol-induced rose microtubule polymerization in vitro and its inhibition by colchicine. *J. Cell Biol.* 99:141–145.

33. Murthy, A. S. N., and M. Flavin. 1983. Microtubule assembly using the microtubule associated protein MAP-2 prepared in defined states of phosphorylation with protein kinase and phosphatase. *Eur. J. Biochem.* 137:37–46.

34. Nicklas, R. B., and D. F. Kubai. 1985. Microtubules, chromosome movement and reorientation after chromosomes are detached from the spindle by micromanipulation. *Chromosoma.* 92:313–324.

35. Oppenheim, D. S., B. T. Haushka, and J. R. McIntosh. 1973. Anaphase motions in dilute colchicine. *Exp. Cell Res.* 79:95–105.

36. Penningroth, S., A. Cheung, K. Olehnik, and R. Koslosky. 1982. Mechanochemical coupling in the relaxation of rigor-wave sea urchin sperm flagella. *J. Cell Biol.* 92:733–741.

37. Pickett-Heaps, J., T. Spurck, and D. Tippit. 1984. Chromosome motion and the spindle matrix. *J. Cell Biol.* 99(1, Pt. 2):137s–143s.

38. Pickett-Heaps, J. D., and D. H. Tippit. 1978. The diatom spindle in perspective. *Cell.* 14:455–467.

39. Pickett-Heaps, J. D., D. H. Tippit, and R. Leslie. 1980. Light and electron microscope observations in two large pennate diatoms *Hantzschia* and *Nitzschia*. 1. Mitosis in vivo. *Eur. J. Cell Biol.* 21:1–11.

40. Pickett-Heaps, J. D., D. H. Tippit, and K. R. Porter. 1982. Rethinking mitosis. *Cell.* 29:729–744.

41. Pollard, T. D., and R. R. Weihing. 1974. Actin and myosin and cell movement. *CRC Crit. Rev. Biochem.* 2:1–65.

42. Reynolds, E. S. 1963. The use of lead citrate at high pH as a electron-opaque stain in electron microscopy. *J. Cell Biol.* 17:208–212.

43. Ris, H. 1949. The anaphase movement of chromosomes in the spermatocytes of the grasshopper. *Biol. Bull.* 96:90–106.

44. Sakai, H. 1978. Isolated mitotic apparatus and chromosome motion. *Int. Rev. Cytol.* 55:23–48.

45. Sakai, H., Y. Hiramoto, and R. Kuriyama. 1975. The glycerol-isolated mitotic apparatus: a response to porcine tubulin and induction of chromosome motion. *Dev. Growth Differ.* 17:265–274.

46. Schliwa, M., R. M. Ezzell, and U. Euteneuer. 1984. Erythro-9-[3-(2-hydroxynonyl)]adenine is an effective inhibitor of cell motility and actin assembly. *Proc. Natl. Acad. Sci. USA.* 81:6044–6048.

47. Soranno, T., and J. D. Pickett-Heaps. 1982. Directionally controlled spindle disassembly after mitosis in the diatom *Pinnularia*. *Eur. J. Cell Biol.* 26:234–243.

48. Telzer, B. R., and L. T. Haimo. 1981. Decoration of spindle microtubules with dynein: evidence for uniform polarity. *J. Cell Biol.* 89:373–378.

49. Tippit, D. H., D. Schulz, and J. D. Pickett-Heaps. 1980. Analysis of the distribution of spindle microtubules in the diatom *Fragilaria*. *J. Cell Biol.* 86:402–416.

50. Tippit, D. H., C. T. Fields, K. L. O'Donnell, J. D. Pickett-Heaps, and D. J. McLaughlin. 1984. The organization of microtubules during anaphase and telophase spindle elongation in the rust fungus *Puccinia*. *Eur. J. Cell Biol.* 34:34–44.

51. Vale, R. D., T. S. Reese, and M. P. Sheetz. 1985. Identification of a novel force-generating protein kinesin involved in microtubule-based motility. *Cell.* 42:32–50.

52. Vale, R. D., B. J. Schnapp, T. Mitchison, E. Steuer, T. S. Reese, and M. P. Sheetz. 1985. Different axoplasmic proteins generate movement in opposite directions along microtubules *in vitro*. *Cell.* 43:623–632.

53. Vallee, R. B. 1980. Structure and phosphorylation of microtubule associated protein 2 (MAP2). *Proc. Natl. Acad. Sci. USA.* 77:3206–3210.

54. Vandre, D. D., F. M. Davis, P. N. Rao, and G. G. Borisy. 1984. Phosphoproteins are components of mitotic microtubule organizing centers. *Proc. Natl. Acad. Sci. USA.* 81:4439–4443.

55. Wordeman, L., K. L. McDonald, W. Z. Cande, F. M. Davis, P. N. Rao, and J. L. Salisbury. 1985. Functional mitotic spindles isolated from the diatom *Stephanopyxis turris* are phosphorylated structures. *J. Cell Biol.* 101(5, Pt. 2):153a. (Abstr.)

56. Wordeman, L., K. McDonald, and W. Z. Cande. 1986. The distribution of cytoplasmic microtubules throughout the cell cycle of the centric diatom *Stephanopyxis turris*: their role in nuclear migration and repositioning the mitotic spindle during cytokinesis. *J. Cell Biol.* 102:1688–1698.

57. Zabrecky, J. R., and D. R. Cole. 1982. Effect of ATP on the kinetics of microtubule assembly. *J. Biol. Chem.* 257:4633–4638.

58. Zimmerman, A. M., and A. Forer. 1981. The isolated mitotic apparatus: a model system for studying mitotic mechanisms. *In* Mitosis/Cytokinesis. A. M. Zimmerman and A. Forer, editors. Academic Press, Inc., New York. 327–336.